

## Local elastic properties of polystyrene nanocomposites increase significantly due to nonaffine deformations

Yaroslav M. Beltukov and Dmitry A. Conyuh 

*Ioffe Institute, Politechnicheskaya Strasse 26, 194021 St. Petersburg, Russia*

Ilia A. Solov'yov \*

*Department of Physics, Carl von Ossietzky Universität Oldenburg, Carl-von-Ossietzky-Strasse 9-11, 26129 Oldenburg, Germany, and Ioffe Institute, Politechnicheskaya Strasse 26, 194021 St. Petersburg, Russia*



(Received 25 July 2021; accepted 17 December 2021; published 11 January 2022)

We investigate the local elastic properties of polystyrene doped with SiO<sub>2</sub> nanoparticles by analyzing the local density fluctuations. The density fluctuations were established from coarse-grained molecular dynamics simulations performed with the MARTINI force field. A significant increase in polystyrene stiffness was revealed within a characteristic range of 1.4 nm from the nanoparticle, while polystyrene density saturates to the bulk value at significantly shorter distances. The enhancement of the local elastic properties of the polymer was attributed to the effect of nonaffine deformations at the length scale below 1 nm, which was further confirmed through the random matrix model with variable strength of disorder.

DOI: [10.1103/PhysRevE.105.L012501](https://doi.org/10.1103/PhysRevE.105.L012501)

Polymer nanocomposites have attracted significant attention due to their unique properties and enormous potential as future materials [1]. Experimental investigations have demonstrated that due to the nanoscale inclusions, polymer nanocomposites could possess tailored mechanical, electrical, and thermal properties, as compared to the pure polymers [2–4]. Among many characteristics, the elastic properties of pure polymers and associated nanocomposites have historically attracted considerable attention [5–7]. It was established that polymer doping with nanoparticles even in small concentrations could lead to significant changes in the elasticity of the host material [8–12]. For example, doping of polymethylmethacrylate with just 3 wt. % of SiO<sub>2</sub> nanoparticles may increase the storage modulus of the nanocomposite by 50% [13].

It is well known that for a homogeneous elastic medium the classical elasticity theory defines the relation between local strain and local stress [14]. In the case of doped polymers, the Eshelby theory can be used to determine the deformation of the nanoparticles and the surrounding medium caused by the macroscopic external stress [15]. The resulting overall stiffness of nanocomposites can then be calculated using the Mori-Tanaka approach [16,17]. However, the Eshelby theory becomes inaccurate once the nanoparticles appear to be of the nanometer scale.

Elastic properties of nanocomposites have also been described by the so-called three-phase model [18]. The model assumes that the structure of a polymer is perturbed around the nanoparticle, which results in an effective interface layer around the nanoparticle with intermediate elastic properties.

Due to the large total surface area of a nanoparticle, the interfacial layer has a strong influence on the overall stiffness of the nanocomposite. However, the properties and the thickness of the interfacial layer are generally unknown and at present the three-phase model was used phenomenologically [19–23].

Here we investigate local elastic properties of a polymer medium surrounding a nanoparticle and consider polystyrene doped with amorphous SiO<sub>2</sub> nanoparticles as an example. The results demonstrate a significant increase of polystyrene local elastic properties in a nanometer-large shell around the nanoparticles, where the internal structure of the polystyrene is only slightly perturbed. To elucidate the role of disorder in the studied system, we have further utilized the random matrix model with variable strength of disorder which permitted us to attribute the observed effect to nonaffine deformations in the polymer [24]. The specific case study illuminates a general and versatile approach that can easily be adapted to the study of arbitrary polymer nanocomposites.

An important property of a polymer nanocomposite is the inhomogeneity of its constituents at a microscopic length scale. The effect becomes especially significant for a polymer matrix since its constituent monomers have a much larger size than the individual atoms. Moreover, since polymers surrounding an embedded nanoparticle are often found in a glassy state, monomers' disorder of positions and orientations makes the polymer matrix even more inhomogeneous.

The presence of disorder leads to the so-called nonaffine deformations under homogeneous external load, which could not be described by a combination of local stretches or shears. Nonaffine deformations play a crucial role in macroscopic elasticity properties and were observed in many disordered solids; examples include metallic glasses [25], polymer hydrogels [26], supercooled liquids [27], silica glass [28]. In the case of Lennard-Jones glass it was shown that the clas-

\*ilia.solovyov@uni-oldenburg.de

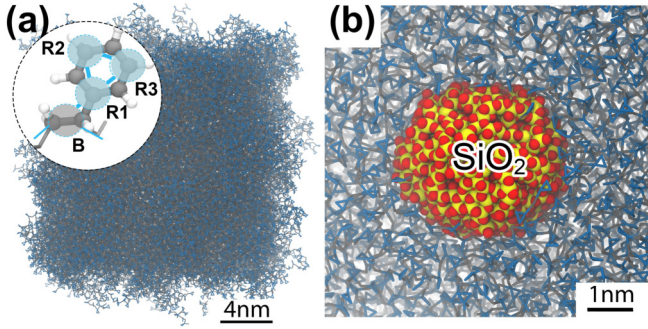


FIG. 1. (a) Characteristic configuration of pure polystyrene inside the simulation box obtained after MD equilibration [33]. Polystyrene is modeled in a coarse-grained representation, where each styrene monomer is represented through four beads denoted as particles R1, R2, R3, and B in the inset. (b) An illustrative configuration of the system featuring an amorphous  $\text{SiO}_2$  nanoparticle embedded into the polystyrene matrix.

sical elasticity theory description fails below a length scale of tens of molecular sizes [29]. Disorder in the polymer matrix is also expected to affect the influence of nanoparticles on the macroscopic elastic properties of the nanocomposite. It was particularly demonstrated recently that nanoparticles in a strongly disordered medium have a stronger impact on the macroscopic elastic properties than nanoparticles in an ordered matrix [30].

To study local elastic properties of polymer nanocomposites, two structures were considered in the present investigation: (i) a reference system of pure polystyrene, as illustrated in Fig. 1(a), and polystyrene doped with an amorphous  $\text{SiO}_2$  nanoparticle, see Fig. 1(b). Pure polystyrene was modeled as a mixture of 216 polystyrene chains consisting of 120 monomers inside a  $17.25 \text{ nm} \times 17.25 \text{ nm} \times 17.25 \text{ nm}$  simulation box. The interaction of coarse-grained polystyrene beads was described by the MARTINI potential [31,32], consistent with earlier studies [32,33]. The polystyrene chains were coarse-grained to permit longer simulations and ensure equilibration of the system. Each styrene monomer was substituted with four coarse-grained beads, as illustrated in the inset of Fig. 1(a). The backbone carbon atoms of polystyrene were modeled through one bead of type B, while three beads of type R represent the styrene side chain. After an extensive equilibration [33], an additional 200-ns-long molecular dynamics (MD) simulation was carried out at 300 K with the use of NAMD 2.13 software [34]. The simulations assumed periodic boundary conditions within the  $NVT$ -statistical ensemble, where the temperature of the system was controlled through the Langevin thermostat with the damping coefficient of  $1 \text{ ps}^{-1}$ .

A single amorphous  $\text{SiO}_2$  nanoparticle with a diameter of 3.6 nm was embedded into the equilibrated polystyrene matrix to model doped polystyrene. Accordingly, the simulation box was increased up to  $17.285 \text{ nm} \times 17.285 \text{ nm} \times 17.285 \text{ nm}$  to accommodate the nanoparticle and preserve the equilibrium density of the polystyrene matrix. An amorphous  $\text{SiO}_2$  nanoparticle was constructed using the programs VMD [35], and MBN STUDIO [36] and embedded into the polystyrene matrix. Since periodic boundary conditions were employed in

the simulation, the studied system is essentially represented by an infinite medium with embedded nanoparticles, which corresponds to polystyrene doping with a mass fraction of 1.6%. This value is consistent with the value typically used for nanocomposites [13]. The van Beest, Kramer, and van Santen (BKS) potential [37] was used to describe the interatomic interactions inside the nanoparticle and its interaction with the polystyrene matrix. The doped polystyrene was simulated for 280 ns using the same parameters as for pure polystyrene. To ensure that the doped polystyrene systems reached equilibrium, and was suitable for the following analysis, the first simulated 80 ns were used to calculate and analyze the spatial distribution of polystyrene density in the simulation box. The approach was identical to the one used previously for pure polystyrene [33] and revealed an equilibrated polystyrene system with  $\text{SiO}_2$  nanoinclusion.

To understand the macroscopic elastic properties of nanocomposites, it is essential to study local elastic moduli around the nanoparticles. One can, for example, analyze stress or strain fluctuations by means of the fluctuation-dissipation theorem [38–42]. The relation between elastic moduli and stress fluctuations contains the Born term, which relies on an involved analysis of the interaction potential between the constituents of the system [43]. On the other hand, the strain fluctuations can readily be obtained directly from MD trajectories.

In this Letter, we analyze the strain fluctuations of a polystyrene nanocomposite and determine its local elastic properties. We focus on studying the density fluctuations, which can be established without the knowledge of the precise equilibrium positions of atoms.

Let us define the relative density of the system at the position  $\mathbf{r}$  and the time instance  $t$  as

$$\xi(\mathbf{r}, t) = \sum_i V_i \phi[\mathbf{r}_i(t) - \mathbf{r}], \quad (1)$$

where  $\mathbf{r}_i(t)$  characterizes the position of the  $i$ th particle and  $V_i$  is the volume of the Voronoi cell attributed to the  $i$ th particle and averaged over the observation time. The smoothing function  $\phi(\mathbf{r})$  reads as

$$\phi(\mathbf{r}) = \frac{1}{(2\pi w^2)^{3/2}} \exp\left(-\frac{r^2}{2w^2}\right), \quad (2)$$

where  $w$  represents the spatial scale of the smoothing function. Thus, the parameter  $w$  determines the spatial resolution of the relative density  $\xi(\mathbf{r}, t)$ . This parameter plays an important role in the evaluation of the local elastic moduli by the analysis of the fluctuations of  $\xi(\mathbf{r}, t)$ . For disordered media, such as polystyrene, larger values of the spatial scale  $w$  lead to a better precision of the elastic properties, but poorer spatial resolution; the resolution is important to analyze the elastic properties of the nanoinclusion and its surrounding medium. In the present Letter, the dependence of local elastic moduli on the spatial scale  $w$  has been analyzed.

The density  $\xi(\mathbf{r}, t)$  in Eq. (1) can be considered as a smoothed three-dimensional histogram with weights  $V_i$ . Since  $V_i$  is the volume attributed to the  $i$ th particle, the density  $\xi(\mathbf{r}, t)$  is expected to be close to unity. Due to the thermal fluctuations, the density deviates from the average value,  $\langle \xi(\mathbf{r}, t) \rangle_t$ ,

where the deviation of density is then defined as  $\delta\xi(\mathbf{r}, t) = \xi(\mathbf{r}, t) - \langle \xi(\mathbf{r}, t) \rangle_t$ .

The thermal fluctuations of density allow determining the local elasticity modulus  $M$  as

$$M(\mathbf{r}) = \left( \theta_3^3 \left( e^{-4\pi^2 w^2 / L^2} \right) - 1 \right) \frac{k_B T \langle \xi(\mathbf{r}, t) \rangle_t^2}{L^3 \langle \delta\xi^2(\mathbf{r}, t) \rangle_t}, \quad (3)$$

where  $\theta_3(x)$  is the third Jacobi theta function,  $L$  defines the dimension of the simulation box,  $k_B$  is the Boltzmann constant, and  $T$  is the temperature of the system. The derivation of Eq. (3) is given in the Supplemental Material [44] using thermal equilibrium analysis of a reference isotropic homogeneous elastic body. For small spatial scales  $w \ll L$  holds and Eq. (3) can be further simplified as

$$M(\mathbf{r}) = \frac{1}{8\pi^{3/2}} \frac{k_B T \langle \xi(\mathbf{r}, t) \rangle_t^2}{w^3 \langle \delta\xi^2(\mathbf{r}, t) \rangle_t}. \quad (4)$$

The elasticity modulus  $M$  is known as the  $P$ -wave modulus and determines the propagation velocity of longitudinal elastic waves as  $v_l = \sqrt{M/\rho}$ , where  $\rho$  is the density [45]. It is related to other elastic moduli through the Poisson's ratio  $\nu$  [46], which for glassy polymers is usually close to 1/3 [47].

The smooth relative density  $\xi(\mathbf{r}, t)$  was computed during the MD simulation of bulk polystyrene and polystyrene with an embedded nanoparticle. In the latter case, the sum in Eq. (1) includes atoms of the nanoparticle. Since the direct calculation of the convolution in Eq. (1) takes considerable calculation time, we use the smooth histogram method described in the Supplemental Material [44].

Figures 2(a)–2(c) show the computed elastic modulus  $M(\mathbf{r})$  for bulk polystyrene obtained for different spatial scales  $w$ . One notes strong spatial fluctuations of the elastic modulus in the case of  $w = 0.4$  nm, while the spatial fluctuations decrease for the larger  $w$  values. The dependence of the mean elastic modulus  $\langle M \rangle$  and the standard deviation  $\delta M$  as a function of the spatial scale  $w$  is presented in Figs. 3(a) and 3(b). With increasing  $w$ ,  $\langle M \rangle$  tends to its macroscopic value and  $\delta M$  decreases. For the investigated values of  $w$  one observes  $\delta M \propto 1/w$ ; in the case of uncorrelated noise one would expect that  $\delta M$  will decrease with the increase of the smoothing length as  $1/w^{3/2}$ . It is thus important to study the correlation function  $C(\mathbf{r}) = \langle (M(\mathbf{r}') - \langle M \rangle)(M(\mathbf{r}' + \mathbf{r}) - \langle M \rangle) \rangle_r$  of the local elastic modulus to determine the relevant correlation length in the system. The obtained correlation function  $C(r)$ , averaged over the different spatial directions in the sample, is presented in Fig. 3 for several spatial scales  $w$ . One can see the exponential behavior of the correlation function  $C(r) \propto \exp(-r/\lambda_c)$  with  $\lambda_c \approx 1.4$  nm. Significant fluctuations of the local elastic modulus for small spatial scales and its correlated behavior make it necessary to study the nanoscale elastic properties in more detail.

Figures 2(d)–2(f) show the elastic modulus  $M(\mathbf{r})$  obtained for polystyrene with an embedded nanoparticle. Far from the nanoparticle, one observes fluctuations of the elastic modulus  $M(\mathbf{r})$  similarly as for bulk polystyrene; see Figs. 2(a)–2(c). Inside the nanoparticle, the elastic modulus is significantly larger,  $M = 70$ – $100$  GPa, corresponding to the typical values for  $\text{SiO}_2$  [45,48] (see the Supplemental Material [44] for more details). It is, however, remarkable that the elastic modulus of

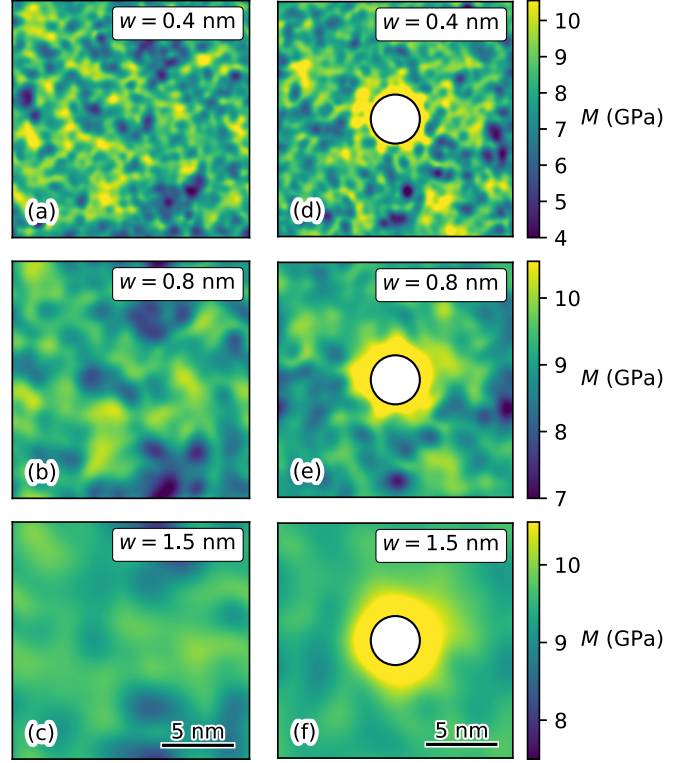


FIG. 2. Spatial distribution of the elastic modulus  $M(\mathbf{r})$  for pure polystyrene (a)–(c) and doped polystyrene sample around a  $\text{SiO}_2$  nanoparticle of 3.6 nm diameter (d)–(f). The results are shown for the central cut plane in the sample (for the doped sample it passes through the center of the nanoparticle). The nanoparticle is shown schematically with a circle. Results are shown for the three spatial scales  $w = 0.4, 0.8,$  and  $1.5$  nm.

polystyrene surrounding the nanoparticle is noticeably larger than the corresponding bulk value. The relative elastic modulus of polystyrene and the  $\text{SiO}_2$  nanoparticle are analyzed in Fig. 4 as a function of distance from the nanoparticle center.

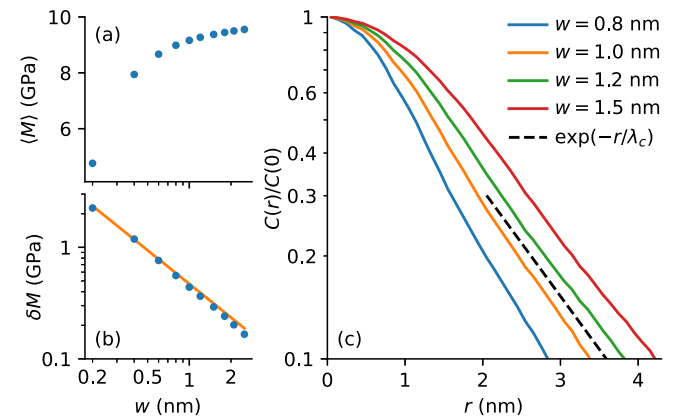


FIG. 3. (a) Mean  $\langle M \rangle$  of the local elastic modulus for the doped polystyrene as a function of the spatial scale  $w$ . (b) Standard deviation  $\delta M$  of the elastic modulus. The line shows the dependence  $\delta M \propto 1/w$ . (c) Correlation function of the local elastic modulus for the four spatial scales  $w = 0.8, 1.0, 1.2,$  and  $1.5$  nm. The dashed line shows the dependence  $\exp(-r/\lambda_c)$ , where  $\lambda_c = 1.4$  nm

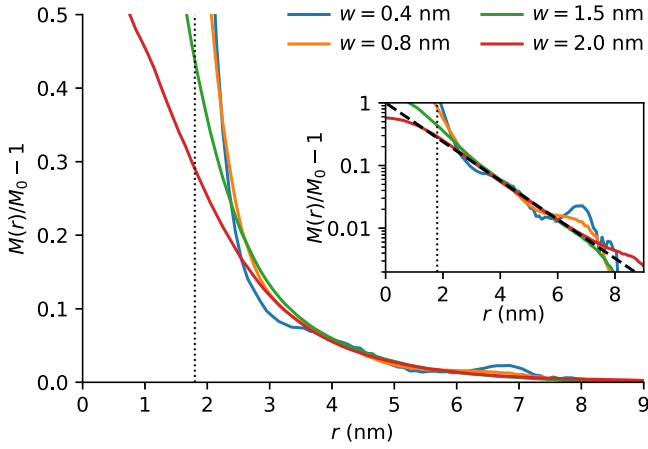


FIG. 4. Relative increase of the elastic modulus  $M$  caused by the  $\text{SiO}_2$  nanoinclusion computed as a function of distance from its center. Results are shown for the four considered spatial scales  $w$ . The vertical dotted line indicates the boundary of the nanoinclusion. The inset shows the same dependence in the logarithmic scale together with an asymptotic function  $\exp(-r/\lambda)$ , where  $\lambda = 1.4$  nm (dashed line).

A 10% enhancement of the elastic modulus is observed for distances up to 1 nm from the nanoparticle surface. This result is not significantly influenced by the smoothing length scale  $w$ , as evidenced in the inset to Fig. 4, which indicates that the observed enhancement of elastic modulus is not related to the smoothing of density fluctuations. Such elastic behavior is consistent with the description obtained from the three-phase model of the nanocomposite [18], however, it is important to discuss the nature of the enhanced elastic properties around the nanoparticle.

The cause of the enhancement in the elastic properties in the vicinity of the nanoparticle can be analyzed through evaluating the density  $\rho(\mathbf{r}) = \sum_i m_i \phi(\mathbf{r} - \mathbf{r}_i)$  separately for the nanoparticle and the polystyrene, as shown in Fig. 5. Here  $m_i$  is the mass of the  $i$ th coarse-grained particle and  $\phi$

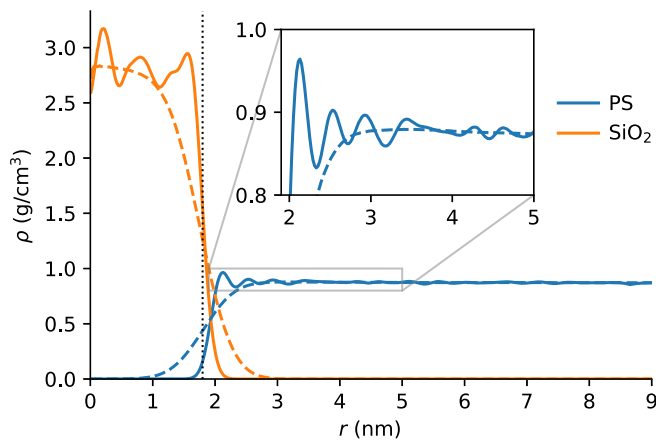


FIG. 5. Radial local density of the  $\text{SiO}_2$  nanoparticle and the polystyrene (PS) matrix. The vertical dotted line marks the boundary of the nanoparticle. Solid and dashed lines show the density for  $w = 0.1$  nm and  $w = 0.4$  nm, respectively. Inset shows a zoom for PS density around the nanoparticle.

is the smoothing function defined in Eq. (2). For the small smoothing value of  $w = 0.1$  nm, one notes clear oscillations of polystyrene density caused by coordination shells of the polystyrene monomers around the nanoparticle. The oscillations vanish for  $w = 0.4$  nm, and the polystyrene density approaches its bulk value with a deviation of less than 1%. At the same time, Fig. 4 demonstrates a much larger deviation of  $M(r)$ , which shows that the enhancement of  $M(r)$  near the nanoparticle is not directly related to the structural changes of the polymer in the vicinity of the nanoparticle. Other structural quantities also exhibit the same behavior near the nanoparticle and in the bulk polystyrene. Volumes of Voronoi cells around individual coarse-grain particles representing the polymer have homogeneous distribution except a narrow layer about 0.5 nm thick around the nanoparticle. Furthermore, the orientation of monomers is isotropic near the nanoparticle as well as in the bulk polystyrene. The detailed analysis of these quantities is presented in the Supplemental Material [44].

In a strongly inhomogeneous medium, the local elastic properties are not completely determined by its local structure but depend on a large volume of the surrounding medium. Indeed, all atoms in the system tend to find new equilibrium positions for any applied macroscopic or microscopic stress. This deviation of equilibrium positions can be described by a continuous function  $\mathbf{u}(\mathbf{r})$ ; however, at the nanometer length scale, each atom has an additional nonaffine displacement  $\mathbf{u}_i^{\text{na}}$ . At the nanoparticle's surface, the nonaffine displacements are suppressed because the nanoparticle is more homogeneous and stiffer than the surrounding polystyrene matrix, leading to different stiffness of the polystyrene matrix in the vicinity of the nanoparticle.

The inset in Fig. 4 shows that the additional stiffness of polystyrene has an exponential behavior  $M(r)/M_0 - 1 \sim \exp(-r/\lambda)$  with  $\lambda = 1.4$  nm, where  $M_0$  is the mean local elastic modulus far away from the inclusion ( $r > 8.6$  nm) and the length scale  $\lambda$  determines the characteristic length scale of nonaffine displacements. The deviation from the exponential law in the inset in Fig. 4 is determined by small fluctuations of the local modulus  $M(r)$ , which remain after averaging of local modulus over a sphere with a given radius  $r$ . The obtained length scale  $\lambda$  coincides with the correlation radius  $\lambda_c$  of the obtained local modulus for the pure polystyrene (Fig. 3). Note that the decay length  $\lambda \approx 1.4$  nm for the shell of higher elastic modulus turns out to be close to the particle radius of 1.8 nm. The result suggests that a more systematic analysis of  $\lambda$  on particle size is called for. Such an analysis is beyond the scope of this investigation as significant computations of polystyrene with nanoinclusions of different sizes would be necessary, and should be completed independently in a followup study.

The effect of disorder on local elastic properties around nanoparticles in an amorphous medium can be further quantified through employing the dimensionless random matrix model [24]. The random matrix model describes many of the general vibrational and mechanical properties of amorphous solids [24,49,50] and is based on the fundamental property that the dynamic matrix is positive definite for a system close to an equilibrium.

In the framework of the random matrix model, the disorder is controlled by the dimensionless parameter  $\mu$ , where  $\mu \gg 1$

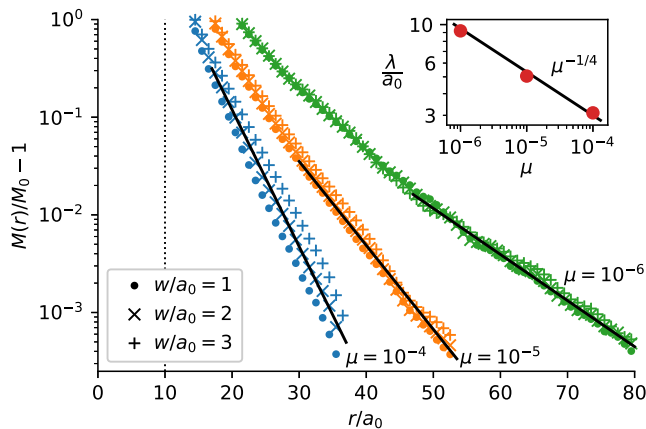


FIG. 6. Relative increase of the elastic modulus  $M$  near the nanoinclusion computed within the random matrix model for different values of the spatial scale:  $w = 1a_0$  (dots),  $w = 2a_0$  (diagonal crosses),  $w = 3a_0$  (vertical crosses). Different colors correspond to different values of the parameter  $\mu = 10^{-4}$ ,  $10^{-5}$ ,  $10^{-6}$ . Dotted line shows the nanoinclusion size  $R_{\text{NP}} = 10a_0$ . Solid lines show the exponential trend  $\sim \exp(-r/\lambda)$  for the corresponding values of  $\mu$ . Inset shows the dependence of the fitted values of  $\lambda$  on the parameter  $\mu$ .

describes the regime with tiny fluctuations of the interaction between atoms; the other regime,  $\mu \ll 1$  describes a strongly disordered amorphous material [24]. To model a disordered medium around the nanoparticle one can consider a simple cubic lattice with the lattice constant  $a_0$  and strong fluctuations of bond strength described by  $\mu \ll 1$ . The nanoparticle is then described as a spherical region with  $R < R_{\text{NP}}$  and  $\mu = \mu_{\text{NP}} = 1$  inside that region. The details of the random matrix model and its analysis are presented in the Supplemental Material [44].

Following the random matrix model, the radial dependence of the calculated elastic modulus  $M(r)$  is presented in Fig. 6 which reveals the exponential dependence of the elastic modulus around the nanoparticle on distance from its center. In the case of a stronger disorder (characterized by the smaller values of  $\mu$ ), one notes a more prominent dependence that is not strongly dependent on the smoothing parameter  $w$ . For each value of the parameter  $\mu$ , one can determine the

length scale  $\lambda$  of the exponential decay of  $M(r)/M_0 - 1 \sim \exp(-r/\lambda)$ , such that  $\lambda \sim \mu^{-\alpha}$  with  $\alpha = 0.24 \pm 0.02$ . The found dependency is close to  $\lambda \sim \mu^{-1/4}$  (see inset to Fig. 6), which is one of the known scaling regimes in the random matrix model [24]. Since the random matrix model requires less computational resources than the MD simulation, it was used to verify whether the thickness  $\lambda$  of the induced elastic shell is influenced by the radius of the nanoparticle. It was revealed that this is not the case but the thickness  $\lambda$  was shown to be affected by the disorder of the surrounding matrix (see the Supplemental Material [44]).

The performed investigation concludes that an exponentially decreasing induced elastic shell is formed around a nanoparticle embedded inside a soft polystyrene matrix. Such a shell increases the effective volume of nanoinclusions inside polymeric materials, which leads to an increase in the effect on the macroscopic elastic properties of nanocomposites.

The resulting elastic properties can approximately be modeled using the three-phase model with the interphase layer thickness  $\lambda \approx 1.4$  nm. The observed enhancement of polystyrene's elastic properties could not be explained by the deviation of its density and other structural properties. The result is consistent with a recent study for boehmite nanolayer in epoxy [51]. We conclude that the increase of elastic properties of the polystyrene matrix was caused by its nonaffine deformations, which are strongly inhomogeneous at the nanometer length scale. This conclusion was supported by the analysis within the random matrix model with variable strength of disorder. We expect the maximum effect on macroscopic elastic properties if a typical distance between nanoparticles is of the order of the length scale  $\lambda$  and the induced elastic shells do not overlap significantly.

The presented results show that detailed elasticity maps at different length scales can be computed by the analysis of the density fluctuations, which can be performed on the fly during an MD simulation. The same analysis can be applied to study local elastic properties in various soft inhomogeneous mediums and liquids as well.

The financial support from the Russian Science Foundation under Grant No. 17-72-20201 is gratefully acknowledged.

- [1] Y. Mai and Z. Yu, *Polymer Nanocomposites*, Woodhead Publishing Series in Composites Science and Engineering (Woodhead Publishing, Cambridge, 2006).
- [2] D. R. Paul and L. M. Robeson, *Polymer* **49**, 3187 (2008).
- [3] A. Vassiliou, D. Bikiaris, K. Chrissafis, K. Paraskevopoulos, S. Stavrev, and A. Docoslis, *Compos. Sci. Technol.* **68**, 933 (2008).
- [4] M. Knite, V. Teteris, B. Polyakov, and D. Erts, *Mater. Sci. Eng.: C* **19**, 15 (2002).
- [5] E. T. Thostenson and T.-W. Chou, *J. Phys. D* **36**, 573 (2003).
- [6] M. A. Rafiee, J. Rafiee, Z. Wang, H. Song, Z.-Z. Yu, and N. Koratkar, *ACS Nano* **3**, 3884 (2009).
- [7] A. Mesbah, F. Zairi, S. Boutaleb, J.-M. Gloaguen, M. Naït-Abdelaziz, S. Xie, T. Boukharouba, and J.-M. Lefebvre, *J. Appl. Polym. Sci.* **114**, 3274 (2009).
- [8] S.-Y. Fu, X.-Q. Feng, B. Lauke, and Y.-W. Mai, *Composites, Part B* **39**, 933 (2008).
- [9] Y. Ou, F. Yang, and Z.-Z. Yu, *J. Polym. Sci., Part B: Polym. Phys.* **36**, 789 (1998).
- [10] H. Wang, Y. Bai, S. Liu, J. Wu, and C. Wong, *Acta Mater.* **50**, 4369 (2002).
- [11] B. Wetzels, F. Hauptert, and M. Q. Zhang, *Compos. Sci. Technol.* **63**, 2055 (2003).
- [12] V. A. Bershtein, O. P. Grigoryeva, P. N. Yakushev, and A. M. Fainleib, *Polym. Compos.* **42**, 6777 (2021).
- [13] D. Stojanovic, A. Orlovic, S. Markovic, V. Radmilovic, P. S. Uskokovic, and R. Aleksic, *J. Mater. Sci.* **44**, 6223 (2009).
- [14] L. Landau, E. Lifshitz, A. Kosevich, J. Sykes, L. Pitaevskii, and W. Reid, *Theory of Elasticity: Volume 7*, Course of Theoretical Physics (Butterworth-Heinemann, Oxford, 1986).

- [15] J. Eshelby, *Proc. R. Soc. London, Ser. A* **241**, 376 (1957).
- [16] T. Mori and K. Tanaka, *Acta Metall.* **21**, 571 (1973).
- [17] Y. Benveniste, *Mech. Mater.* **6**, 147 (1987).
- [18] G. Odegard, T. Clancy, and T. Gates, *Polymer* **46**, 553 (2005).
- [19] F. Bondioli, V. Cannillo, E. Fabbri, and M. Messori, *J. Appl. Polym. Sci.* **97**, 2382 (2005).
- [20] S. Saber-Samandari and A. Afaghi-Khatibi, *Polym. Compos.* **28**, 405 (2007).
- [21] R. Qiao and L. C. Brinson, *Compos. Sci. Technol.* **69**, 491 (2009).
- [22] H. Wang, H. Zhou, R. Peng, and L. Mishnaevsky Jr, *Compos. Sci. Technol.* **71**, 980 (2011).
- [23] J. Amraei, J. E. Jam, B. Arab, and R. D. Firouz-Abadi, *J. Compos. Mater.* **53**, 1261 (2019).
- [24] Y. M. Beltukov, V. I. Kozub, and D. A. Parshin, *Phys. Rev. B* **87**, 134203 (2013).
- [25] R. Jana and L. Pastewka, *J. Phys.: Mater.* **2**, 045006 (2019).
- [26] Q. Wen, A. Basu, P. A. Janmey, and A. G. Yodh, *Soft Matter* **8**, 8039 (2012).
- [27] E. Del Gado, P. Ilg, M. Kröger, and H. C. Öttinger, *Phys. Rev. Lett.* **101**, 095501 (2008).
- [28] F. Leonforte, A. Tanguy, J. P. Wittmer, and J.-L. Barrat, *Phys. Rev. Lett.* **97**, 055501 (2006).
- [29] F. Leonforte, R. Boissière, A. Tanguy, J. P. Wittmer, and J.-L. Barrat, *Phys. Rev. B* **72**, 224206 (2005).
- [30] D. Conyuh, Y. Beltukov, and D. Parshin, *Phys. Solid State* **61**, 1272 (2019).
- [31] S. Marrink, H. Risselada, S. Yefimov, D. Tieleman, and A. de Vries, *J. Phys. Chem. B* **111**, 7812 (2007).
- [32] G. Rossi, L. Monticelli, S. R. Puisto, I. Vattulainen, and T. Ala-Nissila, *Soft Matter* **7**, 698 (2011).
- [33] Y. M. Beltukov, I. Gula, A. M. Samsonov, and I. A. Solov'yov, *Eur. Phys. J. D* **73**, 226 (2019).
- [34] J. C. Phillips, R. Braun, W. Wang, J. Gumbart, E. Tajkhorshid, E. Villa, C. Chipot, R. D. Skeel, L. Kale, and K. Schulten, *J. Comput. Chem.* **26**, 1781 (2005).
- [35] W. Humphrey, A. Dalke, and K. Schulten, *J. Mol. Graphics* **14**, 33 (1996).
- [36] G. B. Sushko, I. A. Solov'yov, and A. V. Solov'yov, *J. Mol. Graphics Modell.* **88**, 247 (2019).
- [37] K. Vollmayr, W. Kob, and K. Binder, *Phys. Rev. B* **54**, 15808 (1996).
- [38] S. Sengupta, P. Nielaba, M. Rao, and K. Binder, *Phys. Rev. E* **61**, 1072 (2000).
- [39] K. Yoshimoto, T. S. Jain, K. Van Workum, P. F. Nealey, and J. J. de Pablo, *Phys. Rev. Lett.* **93**, 175501 (2004).
- [40] M. Tsamados, A. Tanguy, C. Goldenberg, and J.-L. Barrat, *Phys. Rev. E* **80**, 026112 (2009).
- [41] H. Mizuno, S. Mossa, and J.-L. Barrat, *Phys. Rev. E* **87**, 042306 (2013).
- [42] D. M. Sussman, S. S. Schoenholz, Y. Xu, T. Still, A. G. Yodh, and A. J. Liu, *Phys. Rev. E* **92**, 022307 (2015).
- [43] H. Amuasi, C. Heussinger, R. Vink, and A. Zippelius, *New J. Phys.* **17**, 083035 (2015).
- [44] See Supplemental Material at <http://link.aps.org/supplemental/10.1103/PhysRevE.105.L012501> for more details on thermal equilibrium analysis, smooth histogram method, and structural properties of polystyrene around the nanoparticle, which include Ref. [52].
- [45] G. Mavko, C. Chan, and T. Mukerji, *Geophysics* **60**, 1750 (1995).
- [46] G. Mavko, T. Mukerji, and J. Dvorkin, *The Rock Physics Handbook: Tools for Seismic Analysis of Porous Media*, Stanford-Cambridge program (Cambridge University Press, Cambridge, UK, 2003).
- [47] I. Gilmour, A. Trainor, and R. Haward, *J. Appl. Polym. Sci.* **23**, 3129 (1979).
- [48] T. Deschamps, J. Margueritat, C. Martinet, A. Mermet, and B. Champagnon, *Sci. Rep.* **4**, 7193 (2014).
- [49] Y. M. Beltukov and S. E. Skipetrov, *Phys. Rev. B* **96**, 174209 (2017).
- [50] D. A. Conyuh and Y. M. Beltukov, *Phys. Rev. B* **103**, 104204 (2021).
- [51] J. Fankhänel, B. Arash, and R. Rolfes, *Composites, Part B* **176**, 107211 (2019).
- [52] N. Grønbech-Jensen, *Mol. Phys.* **118**, e1662506 (2020).